

Thermomagnetic Optimization of Solenoidal Magnetostrictive Actuators

David C. Meeker^a and David M. Dozor^b

^aFoster-Miller, Inc., 350 Second Avenue, Waltham, MA, USA, 02451

^bMechatronic Technology Co., 23 Chester Rd., Belmont, MA, USA, 02478

ABSTRACT

Magnetostrictive materials often rely on magnetic fields generated through the use of a solenoidal coil. However, the field-generating coil also acts as a source of heat causing thermally induced strains in the magnetostrictive drive element. To insure that the useful magnetostrictive strains are large in comparison with the thermally induced strains, the solenoid may be optimized. This paper presents a simple one dimensional (1-D) magnetic model useful for predicting the magnetic field inside the magnetostrictive drive rod. The advantage of this model is that it can be evaluated very quickly, making it well suited for use in optimization algorithms. A figure of merit is presented that weighs the energy stored in the coil against the power that must be dissipated to maintain the field. With the magnetic model and cost function, the solenoid may be sized to maximize the volume averaged field in the magnetostrictive element per unit of volume averaged dissipated heat in the solenoidal coil. While previous work addressed field/power optimization at the center of air-cored solenoids, the work presented here considers optimization of the average field along a rod of permeable magnetostrictive material. The results indicate that coil quality decreases rapidly if the coil is thinner than optimal, but decreases rather slowly for a thicker than optimal coil.

1. INTRODUCTION

Magnetostrictive materials produce strain in response to an applied magnetic field. A typical geometry for a magnetostrictive actuator consists of a magnetostrictive drive rod encircled by a solenoidal coil. The coil serves not only as a source of magnetomotive force, but also as a source of heat. As an actuator, successful application of a magnetostrictive material relies on the ability to control the mechanical strain through control of the magnetization of the material. The ability to control the magnetization of the material is compromised by the effects of heat. This compromise occurs due to thermal expansion and the pyromagnetic effect. For this reason, coil designs are sought which maximize the volume integral of the magnetic field in the magnetostrictive material while minimizing the volume integral of the heat dissipated by the solenoid which provides the field.

Optimization of air-cored solenoids is well-documented.¹⁻³ In an air-cored solenoid, the solution for the magnetic field along the centerline is fairly straightforward. Although the solution is somewhat complicated, the closed-form analytical solution relies on two important assumptions;

1. There is only an axial component of magnetic field along the centerline (all other components cancel).
2. The relative permeability of the core is unity (the core is not comprised of a magnetizable material).

Due to the construction of solenoidal coils, the first assumption above is quite acceptable. Because magnetostrictive materials are often utilized in the form of a rod with length that is many times greater than the diameter, the centerline field very closely approximates the axial field along the rod. However, since magnetostrictive materials are more magnetically permeable than air, the second assumption is not employed in the present work.

The present paper seeks to optimize coil geometry so as to reduce the required power dissipation while taking into account the effects of the permeable magnetostrictive materials on the magnetic field. This optimization is possible through the use of a volume integral method to rapidly solve for the field in the magnetostrictive material, in combination with a novel figure of merit that balances the energy in the rod with the power required to maintain the field. The result is that the optimal coil shapes in the presence of the magnetostrictive material are somewhat different than the optimal air-cored solenoid shapes previously presented in the literature.

Further author information: (Send correspondence to D.M.Dozor)

D.M.D.: E-mail: dozor@mechatronictech.com

D.C.M.: E-mail: dmeeker@foster-miller.com

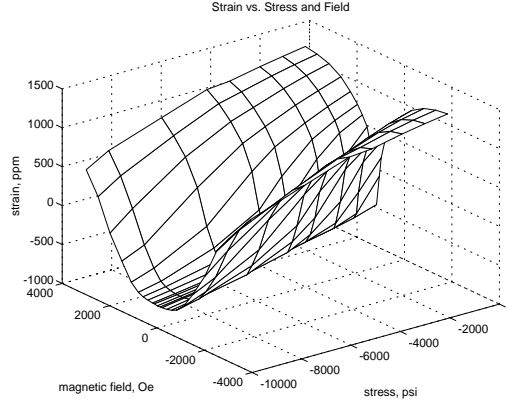


Figure 1. Anhyseteric Strain Surface for FSZM Terfenol-D

2. MAGNETOSTRICTIVE MATERIALS

The size and shape of a magnetostrictive material changes when its state of magnetization is altered. The state of magnetization may be altered by stress, magnetic field, or by changing the temperature (or thermal field). Considering only longitudinal contributions to the thermodynamic potential of a 1-dimensional (1-D) adiabatic magnetostrictive material, the following (vector) constitutive relation may be written;

$$\begin{bmatrix} d\epsilon \\ dB \\ dS \end{bmatrix} = \begin{bmatrix} \left. \frac{\partial^2 G}{\partial \sigma^2} \right|_{H,T} & \left. \frac{\partial^2 G}{\partial \sigma \partial H} \right|_{\sigma,T} & \left. \frac{\partial^2 G}{\partial \sigma \partial T} \right|_{\sigma,H} \\ \left. \frac{\partial^2 G}{\partial H \partial \sigma} \right|_{H,T} & \left. \frac{\partial^2 G}{\partial H^2} \right|_{\sigma,T} & \left. \frac{\partial^2 G}{\partial H \partial T} \right|_{\sigma,H} \\ \left. \frac{\partial^2 G}{\partial T \partial \sigma} \right|_{H,T} & \left. \frac{\partial^2 G}{\partial T \partial H} \right|_{\sigma,T} & \left. \frac{\partial^2 G}{\partial T^2} \right|_{\sigma,H} \end{bmatrix} \begin{bmatrix} d\sigma \\ dH \\ dT \end{bmatrix} \quad (1)$$

Written in terms of the system variables;

$$\begin{bmatrix} d\epsilon \\ dB \\ dS \end{bmatrix} = \begin{bmatrix} \left. \frac{\partial \epsilon}{\partial \sigma} \right|_{H,T} & \left. \frac{\partial \epsilon}{\partial H} \right|_{\sigma,T} & \left. \frac{\partial \epsilon}{\partial T} \right|_{\sigma,H} \\ \left. \frac{\partial B}{\partial \sigma} \right|_{H,T} & \left. \frac{\partial B}{\partial H} \right|_{\sigma,T} & \left. \frac{\partial B}{\partial T} \right|_{\sigma,H} \\ \left. \frac{\partial S}{\partial \sigma} \right|_{H,T} & \left. \frac{\partial S}{\partial H} \right|_{\sigma,T} & \left. \frac{\partial S}{\partial T} \right|_{\sigma,H} \end{bmatrix} \begin{bmatrix} d\sigma \\ dH \\ dT \end{bmatrix} = \begin{bmatrix} Y_{H,T}^{-1} & (d_{33})_{\sigma,T} & \alpha_{\sigma,H} \\ (d_{33})_{H,T} & \mu_{\sigma,T} & i_{\sigma,H} \\ \alpha_{H,T} & i_{\sigma,T} & \left(\frac{C_{H,T}}{T} \right)_{\sigma,H} \end{bmatrix} \begin{bmatrix} d\sigma \\ dH \\ dT \end{bmatrix} \quad (2)$$

Where the thermodynamic potential function G is the Gibbs free energy and U is the internal energy.

$$G = U - \sigma\epsilon - HB - TS \quad (3)$$

The variable ϵ is strain, B is magnetic induction, S is entropy per initial volume, σ is stress, H is magnetic field, and T is absolute temperature. The parameter Y is the elastic modulus, d_{33} is the piezomagnetic coefficient, α is the thermal expansion coefficient, μ is the magnetic permeability, i is the pyromagnetic coefficient, and C is the heat capacity per initial volume. Carman and Mitrovic⁴ have also presented this form of the vector constitutive relations.

Shown in Figures 1 and 2 are surfaces representing the anhyseteric isothermal strain and magnetic induction as functions of stress and magnetic field. The dimension representing temperature is not shown. Engineering actuators are often designed to operate in the linear portions of strain and induction surfaces similar to these.

Consideration of equation (2) indicates that the magnetic induction of magnetostrictive materials depends on the state of stress, field, and temperature. Generally, an increase in temperature causes the induction of these materials to decrease. Since temperature effects occur over relatively long time periods, this work will consider isothermal operation, with the intent of minimizing the heat rejected from the solenoid.

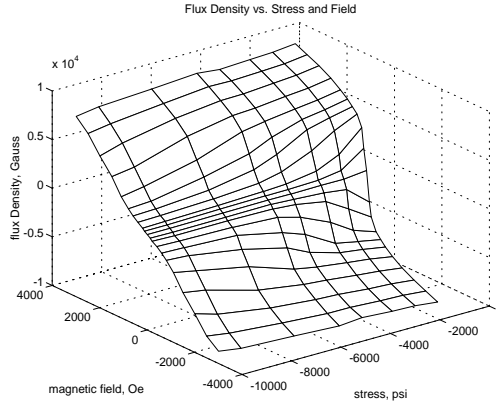


Figure 2. Anhyseretic Induction Surface for FSZM Terfenol-D

3. ENGINEERING APPLICATION OF MAGNETOSTRICTIVE MATERIALS

In recent years, magnetostrictive materials have been designed into useful actuators.^{5–10} This section will focus on the general design methodology and how this relates to the present problem formulation.

In positioning applications, where the deleterious effects of rejected heat are critical, the actuators are generally designed to operate at constant steady-state stress. At constant temperature, equation (2) shows that the magnetic induction of the magnetostrictive material depends only on the field in the magnetostrictive material. This allows the magnetostrictive material to be treated as a general magnetizable solid. The method to be presented may be easily extended to include temperature and stress effects. However, to enhance clarity and provide a design tool for a broad range of applications, temperature and stress effects will be neglected in this paper.

In the design of magnetostrictive actuators, the required material strain and stiffness govern the size of the magnetostrictive drive rod. For the room temperature magnetostrictive material Terfenol-D, the linear region of the strain-field curve at low stresses (<14MPa) is approximately 850ppm. This means that 1.176mm of material length is required for each micron of total strain. Of course greater strains, up to 1600ppm, may be achieved, but very large thermal penalties result.

The stiffness of the magnetostrictive drive rod is designed through selection of the ratio of length to area.

$$K_{rod} = \frac{Y A_{rod}}{l_{rod}} \quad (4)$$

Since the required strain, possibly in conjunction with a stroke amplifier, sets the length of the rod l_{rod} , equation (4) shows that the area of the rod A_{rod} must be selected to achieve the desired stiffness. The rod area A_{rod} in conjunction with manufacturing tolerances, sets the coil inside diameter ID_{coil} . The method for optimizing the coil geometry may take as an input ID_{coil} and provide as outputs the coil outer diameter OD_{coil} , and the length of the coil l_{coil} , which may be longer or shorter than the length of the rod l_{rod} .

4. AIR-CORED, CONSTANT CURRENT DENSITY SOLENOIDS

The work of Montgomery¹ and others^{2,3} focused on developing relationships for air-cored solenoids. Specifically, the work considered analytical and graphical methods for determining the field at various points within solenoids.

Beginning with the Biot-Savart law, expressions for the solenoid central field were derived. Biot-Savart Law prescribes the magnetic field resulting from a “point current” in free space. The magnetic field for an entire coil can then be computed by integrating the magnetic field from each differential piece of current over the entire volume of the coil. Specifically, the Biot-Savart Law is:

$$dH_c = \frac{IdS \times \hat{r}}{4\pi R \cdot R} \quad (5)$$

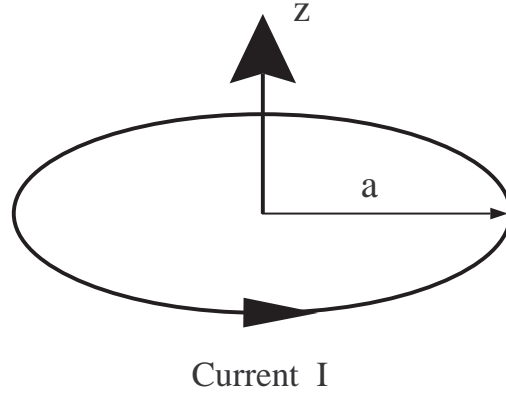


Figure 3. Current loop producing magnetic field

where dH_c represents the differential contribution of a current I to the field produced by the coil of interest. The vector R connects the point at which the current is located to the observer's location.

Equation (5) can be integrated around a loop of wire to obtain the magnetic field of the loop. Such a loop is pictured in Figure 3. The magnetic field of a loop can be integrated to yield the field anywhere with respect to the loop, but this expression is rather complicated.¹¹ Along the centerline of the loop, however, the only component of the magnetic field is directed axially; all other field components integrate to zero. The field intensity, H , along the axis is then:

$$H_{loop}(z) = \frac{Ia^2}{2(a^2 + z^2)^{3/2}} \quad (6)$$

where a denotes the radius of the loop, z denotes the distance from the center of the loop, and I denotes the current in the loop.

The central field of such a loop H_0 may be written:

$$H_{loop}(0) = H_0 = \frac{I}{2a} \quad (7)$$

And equation (6) may be written as;

$$H_{loop}(z) = H_0 \frac{a^3}{(a^2 + z^2)^{3/2}} \quad (8)$$

Integrating the field produced by a solenoidal current sheet in the axial directions, the field at the center of the current sheet solenoid may be represented by the following.

$$H_0 = \frac{NI\beta}{(1 + \beta^2)^{1/2}l_{coil}} \quad (9)$$

Where NI is the magnetomotive force provided by the current sheet.

Montgomery scaled the coil outer radius and half-length by the coil inner radius. In this work, the ratio of coil outer radius to inner radius (or $\frac{OD_{coil}}{ID_{coil}}$) is defined as alpha α . The ratio of the coil half-length to the inner radius (or $\frac{l_{coil}}{ID_{coil}}$) is defined as beta β .

Integration in the radial direction may be performed to derive a central field expression for a finite thickness solenoid of uniform current density:

$$H_0 = J \left(\frac{ID_{coil}}{2} \right) \beta \log \frac{\alpha + (\alpha^2 + \beta^2)^{1/2}}{1 + (1 + \beta^2)^{1/2}} \quad (10)$$

The coil dissipated power may be written as;

$$P = \rho J^2 \int dv_{coil} \quad (11)$$

where ρ in the coil resistivity, and v_{coil} is the coil volume.

From equations (10) and (11), an expression for the central field in terms of the dissipated power may be written in terms of a geometry dependent ‘‘Fabry factor.’’

$$H_o = G(\alpha, \beta) \left(\frac{2P}{\rho ID_{coil}} \right)^{1/2} \quad (12)$$

where the ‘‘Fabry factor’’ is defined as follows.

$$G(\alpha, \beta) = \left[\frac{\beta}{2\pi\beta(\alpha^2 - 1)} \right]^{1/2} \ln \frac{\alpha + (\alpha^2 + \beta^2)^{1/2}}{1 + (1 + \beta^2)^{1/2}} \quad (13)$$

The ‘‘Fabry factor’’ may be plotted in the $\alpha - \beta$ plane. The resulting contours define coils for which a given amount of field is generated per unit of power. By maximizing the ‘‘Fabry factor,’’ a coil geometry may be determined that optimizes the central field of the air-cored solenoid per unit of dissipated power. This value occurs at $(\alpha, \beta) = (3, 2)$. In other words, OD_{coil} should be 3 times ID_{coil} , while the l_{coil} should be 2 times ID_{coil} . This results in a short and stout coil.

It is the objective of this paper to solve a substantially similar problem with the following two exceptions.

1. The core of the solenoid optimized in this paper has relative permeability greater than unity.
2. The volume averaged field in the magnetostrictive core per volume averaged dissipated heat from the solenoid will be maximized.

5. MAGNETIC FIELD DUE TO A CURRENT CARRYING SOLENOID AND A MAGNETIZED SOLID

Computing the axial field of a thin coil is merely the integration of the fields of many differential loops. The case of an infinitely thin coil is useful, in the sense that a cylindrical permanent magnet is equivalent to a volume of air the same size as the magnet surrounded by a sheet of currents. In this case, the current carried by any one differential loop can be represented as $M dz_o$ where dz_o is a differential unit of length axially along the coil, and m is the density of the surface currents. This arrangement is pictured in Figure 4. The convention adopted here is that $z = 0$ at the center of the coil. The length of the coil is l_{coil} .

The integration to find the axial field of the thin coil is:

$$H_{magnet}(z) = \int_{-l_{coil}/2}^{l_{coil}/2} \frac{a^2 m dz_o}{2(a^2 + (z - z_o)^2)^{3/2}} \quad (14)$$

which has the solution

$$H_{magnet}(z) = \frac{m(l_{coil} - 2z)}{\sqrt{4a^2 + (l_{coil} - 2z)^2}} + \frac{m(l_{coil} + 2z)}{\sqrt{4a^2 + (l_{coil} + 2z)^2}} \quad (15)$$

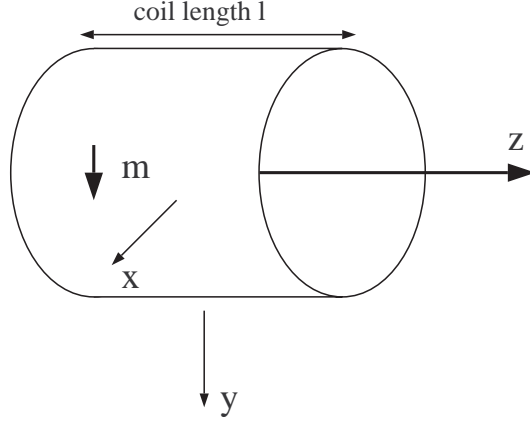


Figure 4. A current sheet surrounding a circular cylinder

To consider a coil of non-zero thickness, equation (15) can be integrated again from the inner radius to the outer radius of the coil to yield the axial magnetic field due to an entire solenoid. If J is the current density carried by the coil, the axial field produced by the coil is:

$$H_{coil}(z) = \left(\frac{J(l_{coil} + 2z)}{4} \right) \log \left[\frac{OD_{coil} + \sqrt{OD_{coil}^2 + (l_{coil} + 2z)^2}}{ID_{coil} + \sqrt{ID_{coil}^2 + (l_{coil} + 2z)^2}} \right] + \left(\frac{J(l_{coil} - 2z)}{4} \right) \log \left[\frac{OD_{coil} + \sqrt{OD_{coil}^2 + (l_{coil} - 2z)^2}}{(ID_{coil} + \sqrt{ID_{coil}^2 + (l_{coil} - 2z)^2})} \right] \quad (16)$$

With equation (16), the field intensity produced along the axis of the coil in air is in an analytical form.

Though equation (15) only describes the magnetic field of the coil in free space, it can be used as the basis for determining the magnetic field when a magnetostrictive core is present. This method is very similar to the Volume Integral method of solving for magnetic fields in inhomogeneous media as described in Ref. 12. The key to this method is the realization that a piece of material of non-unit relative permeability can be represented as an equivalent volume of permanent magnet, having some prescribed magnetization and unit permeability. Mathematically, this equivalence is represented by:

$$B = \mu H = \mu_o(H + M) \quad (17)$$

Magnetization M only exists in volumes that have non-unit permeability. Re-arranging, one can write:

$$(\mu_r - 1)H = M \quad (18)$$

where μ_r is the relative permeability of the material. Defining magnetic susceptibility \mathcal{X} as

$$\mathcal{X} = \mu_r - 1 \quad (19)$$

magnetization can be written in terms of the field intensity H as:

$$M = \mathcal{X}H \quad (20)$$

If the magnetic field is composed of a coil and some magnetized volume, all in free space, the flux density is the sum of a component of flux density from the coil, and a component caused by the magnetized volume. Denoting H_c as the component of the flux intensity from the coil, and H_m the component from the magnetized volume,

$$B = \mu_o(H_c + H_m) \quad (21)$$

Combining equations (17) and (21) yields:

$$\mu_o(H_c + H_m) = \mu_o(H + M)$$

Solving for M and substituting from (20) gives the magnetization at any point as a function of the free-space magnetic field of the coil, and the free space field of the magnetized volume:

$$M = \left(\frac{\mathcal{X}}{1 + \mathcal{X}} \right) (H_c + H_m) \quad (22)$$

Equation (22) is the mechanism for solving the field inside the magnetostrictive drive rod. Since the drive rod lies on the axis of the coil, the H_c component can be obtained via (16). To obtain H_m , a reasonable approximation is to break the magnetostrictive rod into a number of segments, each of which has a constant (but unknown) magnetization. Equation (15) can then be used to obtain the axial field from any particular segment of the rod.

Equation (22) can be used to describe the magnetization at the center of any particular segment of the rod:

$$M(z_i) = \left(\frac{\mathcal{X}}{1 + \mathcal{X}} \right) \left[H_{coil}(z_i) + \sum_{j=1}^n M(z_j) h_{magnet}(z_i - z_j) \right] ; \quad i = 1 \dots n \quad (23)$$

where h_{magnet} is the magnetic field from a uniformly magnetized cylinder per unit of magnetization, obtained by dividing H_{magnet} by m :

$$h_{magnet}(z) = \frac{l - 2z}{\sqrt{4a^2 + (l - 2z)^2}} + \frac{l + 2z}{\sqrt{4a^2 + (l + 2z)^2}} \quad (24)$$

and where n represents the number of segments in the rod. Since equation (23) can be written for each segment in the rod, this equation represents n linear equations for n unknown M_i ; these equations can be solved to yield the magnetization of every segment in the rod. Once the magnetization is known, the field in the rod is available simply by dividing the magnetization by \mathcal{X} .

The power of this method over, for example, the finite element method, is that only the rod of magnetostrictive material need be discretized. There is no need to solve for the field in the air as well (although the field in the air can be obtained with the present method by Biot-Savart once the magnetization is known). Breaking the rod into 100 segments is often more than enough to accurately solve for the field intensity, and the problem solution takes fractions of a second to solve. Many different coil geometries can be investigated automatically and in a short amount of time.

6. DEFINITION OF COIL OPTIMALITY

To optimize coil geometry, some definition of optimality must be developed. In section 4, the ‘‘Fabry factor’’ was used to represent an optimal solenoid geometry. This optimization considered maximization of the central field of an air-cored solenoid per unit of dissipated power.

In the present case, however, the problem is a bit more subtle. Not only the center of the coil is of interest, but H along the entire length of the rod is important. In this work, where the room temperature magnetostrictor Terfenol-D has been applied, the metric for quantifying coil performance will be denoted by the *Terfenol time constant*:

$$\tau_{terf} = \frac{(1/2)\mu H_{avg}^2 v_{terf}}{\rho v_{coil} J^2} \quad (25)$$

Which is loosely interpreted as the magnetic field energy stored in the Terfenol-D drive rod divided by the power required to produce this field. This figure of merit has units of seconds.

A ‘‘good’’ coil should have a high τ_{terf} . Optimizing τ_{terf} implies that the highest average field is achieved in the Terfenol-D for a given amount of loss in the coil.

7. OPTIMIZATION OF COIL GEOMETRY

With a theoretical foundation for computing the field in the magnetostrictive core and a definition of coil optimality defined, a coil geometry may be optimized. To perform this task, a short computer program was written in *C* which sets up and solves equation (23) for a coil and a magnetostrictive rod of prescribed dimensions. The outputs of the program are the dimensions of the coil, the associated Terfenol time constant τ_{terf} , and a profile of H along the rod in units of Amp/Meter.

Optimal coil geometries were computed for three rod sizes of interest in the present work. All Terfenol-D rods considered are 15 mm long and have a relative permeability of 8. The outer diameters considered were 1.5, 2, and 2.5 mm. The rods are assumed to be centrally positioned in the axial direction with respect to the coil (no axial offset).

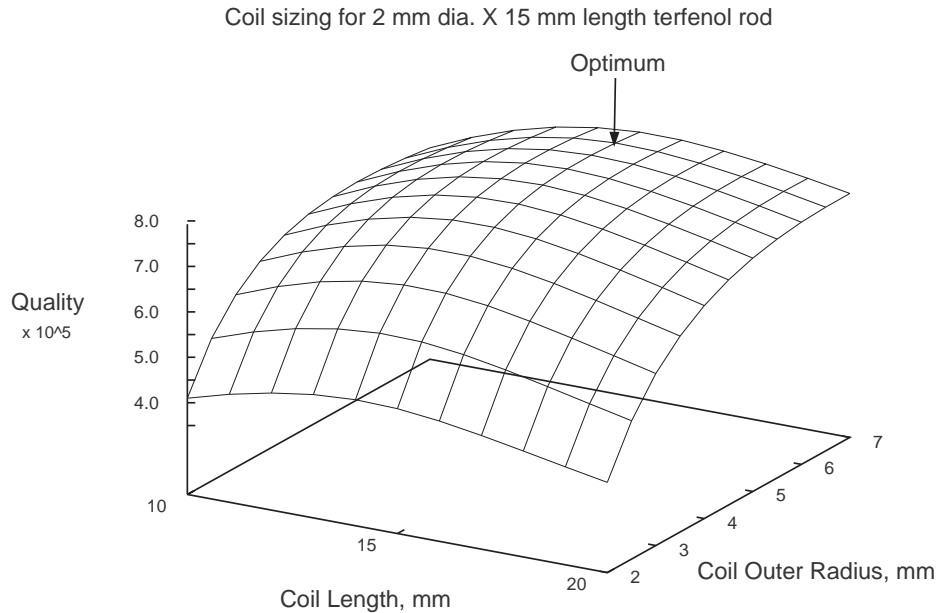


Figure 5. Coil Optimization for a 2 mm diameter Terfenol-D rod

For the optimization, the coil inner diameter was assumed to be the same as the rod outer diameter, and the coil's outer diameter and length were chosen to optimize τ_{terf} . In each case, there is a clearly optimal configuration with respect to τ_{terf} . For the case of the 2 mm rod, the surface created by various values of coil outer diameter and length is pictured in Figure 5.

From the figure, the optimal coil length is approximately, but not, equal to the rod length. There is a clear optimal outer radius and coil quality decreases rapidly if the coil is thinner than optimal, but decreases rather slowly for a thicker than optimal coil. The dimensions for each optimized coil are presented in Table 1.

Rod OD, mm	Coil OD, mm	Coil Length,mm	τ_{terf} , sec.
1.5	10.0	14.8	$5.7(10^{-5})$
2.0	11.6	15.1	$7.9(10^{-5})$
2.5	13.2	15.4	$9.8(10^{-5})$

Table 1. Optimal coil geometries.

For the optimal cases, the field inside the Terfenol-D rod is shown in Figures 6-8. In each case, an interesting qualitative feature is that the field intensity with the Terfenol-D is slightly less than the field intensity without the Terfenol-D. In addition, field intensity at the end of the coil in the absence of the Terfenol-D is about 1/2 of the

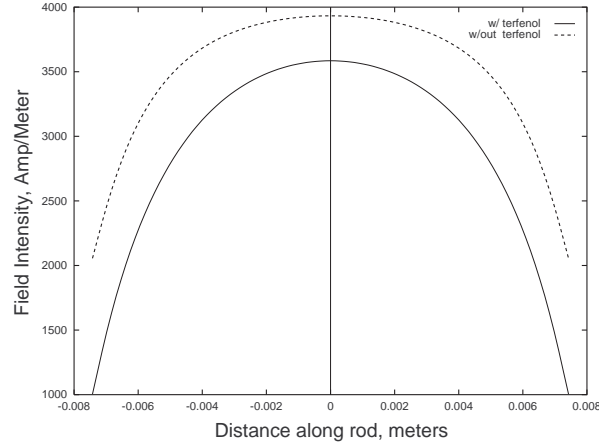


Figure 6. H resulting from 1 MA/m^2 coil current for a 1.5 mm rod.

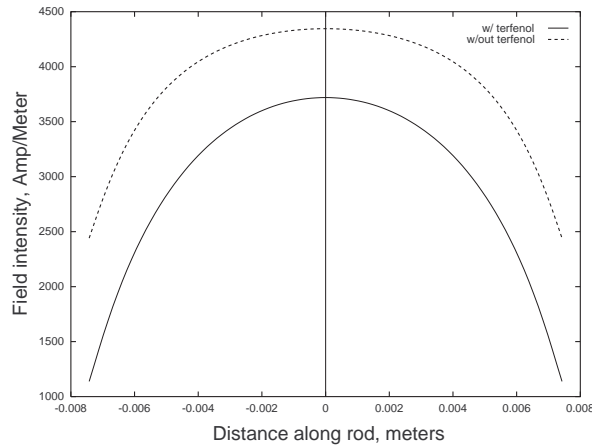


Figure 7. H resulting from 1 MA/m^2 coil current for a 2 mm rod.

value at the center of the coil. With the Terfenol-D, the field intensity at the end of the rods falls to about 1/4 to 1/3 of the center value. Each of the following plots represents the field produced in the Terfenol-D by a 1MA/m^2 coil current. The field intensity for the optimal coils with and without the Terfenol-D are presented in Figures 6-8.

8. CONCLUSIONS

A volume integral model of a solenoid with a magnetostrictive core has been developed. This model readily lends itself to solution via a short computer code. A definition for optimal coil geometry was developed that trades off the average level of field intensity developed in the magnetostrictive drive rod with the power dissipation that is required to create the field intensity. This cost function is denoted τ_{terf} . Using a code that discretizes the drive rod and solves the volume integral formulation, optimal coil geometries were found for some specific rod sizes. Plots were presented that show the qualitative characteristics of the optimization on τ_{terf} .

The 1-D character of magnetostrictive drive rod model is good in the sense that it can easily be incorporated into an elaborate, yet manageable, dynamic model of the magnetostrictive actuator. It would be simple to include the effects of a multiple coil arrangement, or to add magnetization to the rod due to applied stress and/or changing temperature.

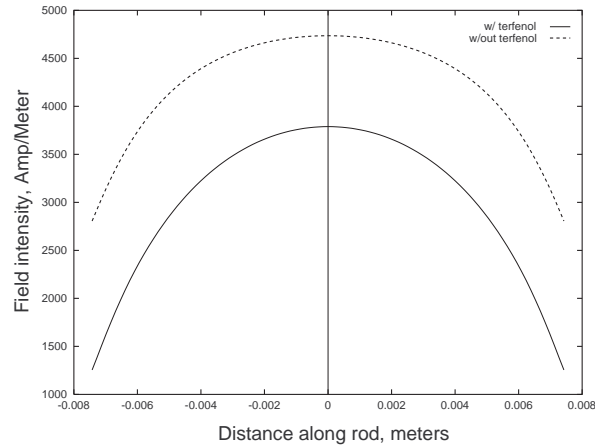


Figure 8. H resulting from 1 MA/m^2 coil current for a 2.5 mm rod.

REFERENCES

1. D. Bruce Montgomery, *Solenoid Magnet Design*, Wiley-Interscience, New York, 1969.
2. Fabry, *Eclairage Electrique*, 17:133, 1898.
3. J. D. Cockcroft, *Phil. Trans. Roy. Soc.*, 227:317, 1928.
4. Carman, G.P. and M. Mitrovic. "Nonlinear Constitutive Relations for Magnetostrictive Materials with Applications to 1-D Problems", *Journal of Intelligent Material Systems and Structures*, 6:673-683.
5. Anjanappa, M. and Bi, J "A Theoretical and Experimental Study of Magnetostrictive Mini-Actuators." *Smart Materials and Structures*, 3(1994) pp. 83-91.
6. Dozor, D.M. "Magnetostrictive Wire Bonding Clamp for Semiconductor Applications: Design, Modeling, and Experiments." *SPIE Symposium on Smart Structures and Materials*, 3326:516-526, 1998.
7. Dozor, D.M., Engel, B.B., Kiley, J.E. "Modeling, Optimization, and Control of Magnetostrictive High Force to Mass Ratio Reaction Mass Actuators." *SPIE Symposium on Smart Structures and Mat'ls*, 3044:370-381, 1997.
8. Dozor, D.M., "Ultra-precision Positioning Devices for Semiconductor Lithography", presented at the 1996 ARPA Adv. Lithography Review, Sarasota, FL and the 1997 SPIE Symposium on Smart Structures, San Diego, CA.
9. Pratt, J. and Flatau, A.B.. "Development and Analysis of a Self-Sensing Magnetostrictive Actuator Design." *Journal of Intelligent Material Systems and Structures*, 6(5):639-648, 1995
10. Wang, W. and Busch-Vishniac, I., 1992. "A High Precision Micropositioner Based on Magnetostriction Principle", *Rev. Sci. Instrum.*, 63(1):249-254.
11. Jackson, J. D., *Classical Electrodynamics*, 2nd ed., Wiley, New York, 1975.
12. Hoole, S. R. H., *Computer-Aided Analysis and Design of Electromagnetic Devices*, Elsevier, New York, 1989.